Phase transitions of hydrogen in quasi-two-dimensional vanadium lattices

2001 J. Phys.: Condens. Matter 13 1685

(http://iopscience.iop.org/0953-8984/13/8/306)

INSTITUTE OF PHYSICS PUBLISHING JOURNAL OF PHYSICS: CONDENSED MATTER

J. Phys.: Condens. Matter **13** (2001) 1685–1698 www.iop.org/Journals/cm PII: S0953-8984(01)18870-3

Phase transitions of hydrogen in quasi-two-dimensional vanadium lattices

Stefan Olsson[1], **Peter Blomquist**[2] **and Björgvin Hjörvarsson**[1,3]

[1] Materials Physics, Royal Institute of Technology, 100 44 Stockholm, Sweden
[2] Department of Physics, Uppsala University, 751 21 Uppsala, Sweden

E-mail: bjorgvin@matphys.kth.se (B Hjörvarsson)

Received 5 November 2000, in final form 12 January 2001

Abstract

The influence of the strain state on the thermodynamics of hydrogen in quasi-two-dimensional potentials is reported. The host lattice is V embedded in Fe in the form of a Fe/V(001) superlattice, which represents a strongly confined absorption potential extending over just 13 monolayers. $\Delta\bar{H}_{\mathrm{H}}$ and $\Delta\bar{S}_{\mathrm{H}}$ for the continuous solubility region are calculated from the measured isotherms. Two phase transitions are observed for atomic ratios up to $c = 1$ in the temperature region 50–300 °C. The first transition occurs in the range $0.03 \leqslant c \leqslant 0.07$, and shows a Curie–Weiss behaviour. No corresponding phase boundary exists in bulk vanadium hydrides. The second transition, at $c \simeq 0.35$ and $T < 150$ °C, exhibits large hysteresis and involves an ordering not previously observed in thin vanadium layers. The site blocking at low concentrations scales linearly with the initial strain and yields a blocking concentration of $c = 0.083(1)$ at zero strain, as compared to 0.415(9) in bulk V. This difference is ascribed to the finite-size of the host lattice.

1. Introduction

Hydrogen (H) in thin metal (M) films and superlattices has recently attracted considerable attention. Not only do thin films provide an arena for investigations of fundamental properties of hydrogen in materials, but also hydrogen can be used to alter the physical properties of the host lattice. For example, a number of researchers [1, 2] have demonstrated both optical and magnetic tuning. The finite extent and the strain state of extremely thin films are expected to strongly affect the thermodynamics of the hydrogen absorption. Hence investigations of hydrogen in thin films and superlattices serve a fundamental as well as a technological purpose.

Wagner and Horner [3] have proposed a theory which describes the $\alpha \rightarrow \alpha'$ transitions of H in coherent metal lattices. They especially considered the dependence of the H–H interaction on the elastic boundary conditions. This peculiar behaviour of the H–H interaction in the coherent state can be understood if one takes into account the coherent condition, which hampers

[3] Author to whom any correspondence should be addressed.

0953-8984/01/081685+14$30.00

rapid variations in the H density. Close to and below the critical temperature for the lattice-gas → lattice-liquid transition, repulsive energy is stored in the form of coherence stresses. The interaction energy can in this case be decomposed into density modes. Modes with a wavelength comparable to the sample size are sensitive to the elastic boundary conditions. When the extent of the hydrogen-absorbing material is much smaller than the density modes observed in the bulk, a strong influence on the phase boundaries is expected. Hence, the extent of thin absorbing films is expected to strongly influence the interaction. The influence of the elastic boundary conditions on the H–H interaction and analogies to electrostatic problems have been qualitatively discussed by Alefeld [4, 5].

The existence of shape-dependent density modes has been verified in experiments [6, 7]. It is important to emphasize that a completely coherent or incoherent phase separation is an idealization that will never be completely achieved in experiments. The actual state of a real crystal is always a mixture between coherent and incoherent regions. As the realization of a coherent phase transition is intimately related to the number of lattice defects and dislocations, the refined techniques of crystal growth open up the possibility to examine the details of coherent phase transitions of H in metals.

The effects of reduced dimensionality and strain state on the H–H interaction have recently been explored by means of thermodynamic investigations of H in Mo/V and Fe/V superlattices [8, 9]. The solution of H in Mo and Fe is endothermic, while it is exothermic in V. At equilibrium, the H atoms are therefore confined in the V layers, which can be made as thin as one monolayer (ML). Furthermore, since the differences in lattice parameter of the constituents generate biaxial strain in the layers, the initial strain state of the hydrogen-containing layers can be tuned by varying the thickness and constituents of the hydrogen-free layers. The influence of the initial strain state of the V lattice on the elastic interaction has proved to be huge in the concentration region $0.1 \leqslant c(\mathrm{H/V}) \leqslant 0.5$ (H/V is the H–V atomic ratio). On changing the biaxial strain state of V from tensile (Mo/V) to compressive (Fe/V), the H–H interaction changes sign from attractive to repulsive [10]. Furthermore, the strain state is inferred to change the site occupancy: T_i ($i = x, y, z$) in Mo/V and O_z in Fe/V.

In this article, solubility isotherms, for 50–300 °C and $c = 0$–1, of H in four different Fe/V(001) superlattices are presented and the influence of the initial strain state of the H-absorbing layers on the thermodynamics of H absorption is discussed. The extent of the absorbing layer is the same for all of the samples (13 ML), allowing a separation of the finite-size effects and the influence of the strain state.

2. Experimental details

2.1. Sample growth

The Fe/V superlattices were grown in a three-target magnetron sputtering system with a base pressure of 10^{-9} mbar. The polished MgO(001) substrates ($10 \times 10 \times 0.5$ mm^2) were all from the same batch and ultrasonically cleaned in ethanol, iso-propanol and acetone, before being subjected to *in situ* annealing at 700 °C for 60 minutes. The sputtering gas was argon (99.9999%). The targets were Fe (99.95%), V (99.7%) and Pd (99.95%). The sputtering-gas pressure was 6.7 mbar and the substrate temperature was 330 °C. The samples were grown at a floating potential and rotated at ≃30 rpm during deposition. After the deposition of the superlattices, they were capped with Pd to avoid oxidation and enhance the kinetics of the hydrogen uptake.

It is possible to tune the strain state of the H-absorbing layer (V) by altering the thickness of the hydrogen-free layer (Fe). The difference in lattice parameter between Fe ($a_{\mathrm{Fe}} = 2.87$ Å)

and V ($a_V = 3.03$ Å) will produce biaxial compressively strained V layers. The average in-plane lattice parameter can be approximated as

$$a_{\parallel} \simeq \frac{L_{Fe}a_{Fe} + L_V a_V}{L_{Fe} + L_V} \tag{1}$$

where L_{Fe} and L_V are the thicknesses of the Fe and V layers respectively. Three conditions have to be fulfilled for successful use of this approximation: linear elasticity theory has to be applicable, the elastic constants of the constituents must be similar and finally the stress relaxation must be small. The first condition is fulfilled since the misfit between the lattice parameter of Fe and V is moderate. Birch *et al* [12] measured the relaxed lattice parameter in Mo/V superlattices and were not able to resolve any significant effect of the different elastic constants of Mo and V lattices. The difference in the elastic constants of Fe and V is even smaller; hence the second condition is fulfilled. X-ray studies of Fe/V superlattices have proved that above a critical thickness of the V layers ($\simeq$23 Å), the dislocation density increases substantially. The thickness of the V layers in this study is well below this value; consequently the third assumption is satisfied.

Each of the four different superlattices used in this study consists of 30 Fe/V bi-layers. The thickness of the Fe layers is varied among the samples: $L_{Fe} = 3$, 6, 9 and 13 ML, while the thickness of the V layers is equal for all of the samples: $L_V = 13$ ML. Using (1), the biaxial compressive strain in the V layers is $\epsilon_{xx} = \epsilon_{yy} = -0.99$, 1.67, -2.16 and -2.64% respectively, where the x- and y-directions are parallel to the film plane. Keeping the thickness of the V layers constant ensures that the contributions from finite-size effects and the electronic boundary conditions on the thermodynamic properties are close to equal for all of the samples.

The samples were characterized by conventional low- and high-angle XRD analysis. Typical results are illustrated in figures 1(a) and 1(b). As seen in figure 1(a), the total thickness of the Fe(9 ML)/V(13 ML) (001) sample is well defined, giving rise to a number of rapid oscillations, visible up to 9°. Six superlattice peaks are seen in the range 0 to 17°. Only a minute increase of the peak width is observed, indicating a well defined repeat distance. The second-order peak is faint due to the thickness ratio of the constituents. The high-angle XRD data are shown in figure 1(b), where the Bragg peak of the film is indicated by 0 and the superlattice satellites by $\pm x$. The FWHM of the (002) peak in the virgin sample is 0.46°, and the FWHM of ω is 0.6744°. Hence, the samples are of the expected quality, as described by Isberg *et al* [13]. The Fe(9 ML)/V(13 ML) sample was investigated after all other measurements were performed. The treatment included cooling the fully loaded sample to $\simeq$77 K. The sample quality decreased somewhat, as expected, mostly due to the cooling cycle. The FWHM of the ω-scan around of the (002) peak increased from 0.6744° to 0.7033°.

2.2. Hydrogen uptake and thermodynamic considerations

The temperature at the surface of the sample was controlled and read by a Eurotherm 94c temperature controller with an accuracy of 1 °C. A 0–1 bar CCM pressure gauge monitored the gas pressure with an accuracy of 0.1% of full scale. The high-purity hydrogen gas used in the experiment was further purified in a two-step process: firstly, using a West Associates ULTRAPURE gas purifier, and thereafter by means of an absorption in a metal hydride, which also served as a store for purified hydrogen gas. Ordinary four-probe *in situ* resistivity measurements were performed, using a Stanford Research 830 lock-in amplifier to register the resistivity change during hydrogen loading. Before any measurements were performed, the chamber was evacuated to below 10^{-8} mbar, while baking the sample stage. Additional removal of impurities was achieved by flushing the chamber several times with hydrogen. The partial pressures of all gases, except hydrogen, were typically below 10^{-11} mbar during the

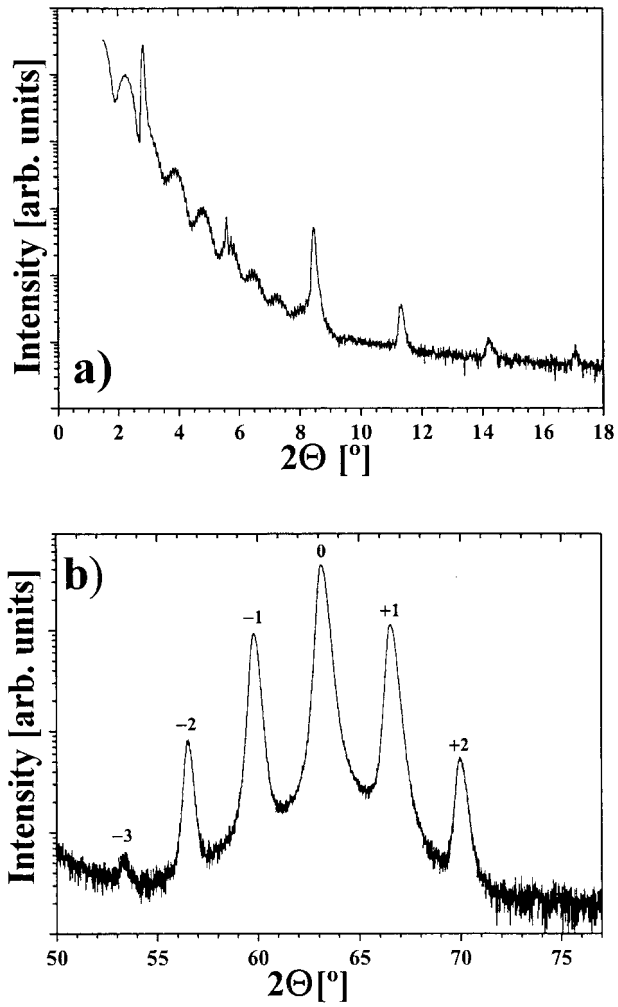

Figure 1. XRD measurements of the virgin Fe(9 ML)/V(13 ML) superlattice. (a) Low-angle reflectivity data. The finite-size oscillations are noticeable up to 9°, and six low-angle superlattice peaks with fairly constant width are visible. The results indicate a well defined total thickness and repeat length; for a discussion on the structural quality, see Isberg *et al* [13]. (b) A high-angle XRD pattern. The Bragg peak of the film is indicated by 0 and the superlattice satellites by $\pm x$.

experiments. The isotherms of H in the four superlattices were thereafter measured with a stepwise increase of the hydrogen-gas pressure from 1 mbar to 1 bar, keeping the temperature constant. The time required to reach equilibrium at each step was typically of the order of ten seconds. Eight isotherms for each sample were measured in the temperature interval 50–300 °C (±1 °C).

The relation between the change in resistivity and the hydrogen concentration was established by measuring the maximum hydrogen uptake at room temperature. The determination was performed at the Tandem accelerator at Uppsala University, using the $^{1}H(^{15}N, \alpha\gamma)^{12}C$ nuclear reaction. After the samples were mounted on a sample stage cryostat, the pressure was allowed to decrease to the low 10^{-9} mbar range. Thereafter, the samples were exposed, *in situ*, to 1 bar of hydrogen gas at room temperature (293 ± 1 K). While exposed to

hydrogen, the samples were rapidly cooled, by filling the cryostat with liquid nitrogen. The scattering chamber was evacuated while cooling, allowing the samples to reach a temperature below 80 K. The extremely slow kinetics of the hydrogen absorption–desorption process at this temperature enables measurements to be made on samples with catalytic overlayers, which at room temperature would desorb the hydrogen upon evacuation.

3. Results and analysis

3.1. Hydrogen induced resistivity change

A typical behaviour of the resistivity change during loading is shown in figure 2. $\Delta R/R_0\big|_{\max} =$ 0.322(5), 0.391(5), 0.458(2) and 0.597(7) for the superlattices with $L_{\mathrm{Fe}} = 13$, 9, 6 and 3 ML respectively. The asymptotic behaviour of $\Delta R/R_0$ during loading is in accordance with a previous study of H in Fe/V superlattices [8]; i.e. the resistance increases continuously in the range $0 < c \leqslant 1$. The hydrogen-induced resistivity change in both thin V films and in Mo/V superlattices has a maximum around $c \simeq 0.5$. At concentrations above 0.5, the resistivity decreases with increasing concentration. The apparent departure from this behaviour for the present samples can be partially understood if one considers the initial band structure of the superlattices and the changes caused by the presence of H [14]. The density of states is modified as well as the difference in the Fermi energy of the superlattice constituents. However, the details are not fully explored and are beyond the scope of the current communication. Instead of considering the different contributions, we have simply used a truncated power series to describe the changes:

$$\frac{\Delta R}{R_0} = f(c_{\mathrm{r}}) = Ac_{\mathrm{r}} + Bc_{\mathrm{r}}^2 \tag{2}$$

where $c_{\mathrm{r}} = c/c_{\max}$. c and $c_{\max}$ are the actual atomic ratio and the geometrically limiting value, respectively. Relation (2) has been verified by previous measurements of H in

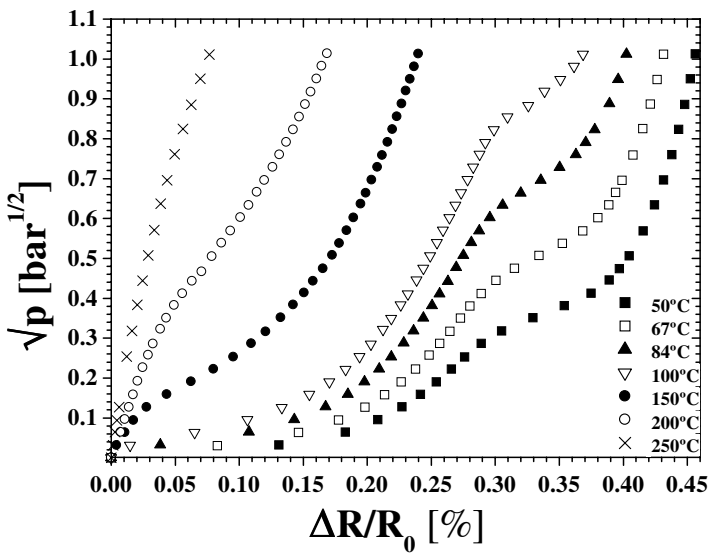

Figure 2. The change of the relative resistance (R_0 is the resistance at 50 °C without hydrogen) during loading of a Fe(6 ML)/V(13 ML)(001) superlattice. The biaxial compressive strain of the V layers is $\epsilon_{xx} = \epsilon_{yy} = -1.67\%$.

superlattices [9, 15]. Here the constants, A and B, are determined by the conditions at the extreme value:

$$f(c_r = 1) = \left.\frac{\Delta R}{R_0}\right|_{max} \tag{3}$$

and

$$f'(c_r = 1) \simeq 0. \tag{4}$$

Condition (3) is self-evident, for the concentration range of interest. On the basis of previous experiments [15], the first derivative is determined to be approaching zero when $c_r \to 1$. Furthermore, at high pressures, $\partial R/\partial(\ln p)$ approaches zero. Accepting proportionality between concentration and the logarithm of the pressure (which holds in a small pressure range) implies thereby condition (4). The estimated maximum error is smaller than 20% of the value in the concentration range of interest, and approaches zero when $c_r \to 0$. Applying the conditions (3) and (4) to expression (2) yields

$$\frac{\Delta R}{R_0} = c_r(2 - c_r)\left.\frac{\Delta R}{R_0}\right|_{max}. \tag{5}$$

The saturated concentration, c_{max}, is obtained by nuclear resonance techniques as described above and the results are presented in table 1. No concentration gradients were observed in the samples, besides those expected at the vacuum and the substrate boundaries. Experiments have shown that the V layers, which are close to the Fe–V interface, contain negligible amounts of hydrogen in the concentration range $c < 0.5$ [8]. At higher concentration, hydrogen begins to populate the interface region. The extent of the hydrogen-depleted region depends on the thickness of the Fe layer. In table 1 we have accounted for this using a first-order approach: we have assumed completely depleted interface regions with an extent of 3 ML in the Fe(9 ML)/V(13 ML) and Fe(6 ML)/V(13 ML) samples and of 2 ML in the Fe(3 ML)/V(13 ML) sample. By using adequate population models, a full description of the concentration distribution can be obtained. However, as the actual measurements are solely aimed at determining the maximum concentration in the samples, these details are omitted here. For a full discussion on the interface models, see reference [16]. In conclusion, the maximum concentration in the interior region corresponds to $c_{max} = 1$; however, the average concentration in the V layers depends on the relative ratio of L_{Fe} and L_V.

Table 1. Results from nuclear resonance analysis, including the hydrogen-to-metal atomic ratio, $\langle H/M\rangle$, average hydrogen-to-V atomic ratio, $\langle H/V\rangle_{av}$ and, finally, the deduced concentration in the interior region, $\langle H/V\rangle_{int}$, assuming interface regions three (*) or two (**) monolayers (ML) thick. This is a somewhat simplified view of the population at the surfaces; see Hjörvarsson *et al* [11, 16] for details.

L_{Fe} (ML)	$\langle H/M\rangle$	$\langle H/V\rangle_{av}$	$\langle H/V\rangle_{int}$
9	0.30 ± 0.02	0.50	0.96*
6	0.36 ± 0.02	0.53	0.98*
3	0.58 ± 0.02	0.72	1.04**

3.2. Thermodynamics

The measured solution isotherms of hydrogen in the different Fe/V superlattices are presented in figure 3. The resistance change during loading is completely reversible for all samples; i.e. the resistance returns to the initial value, within the experimental precision ($\ll 0.1\%$),

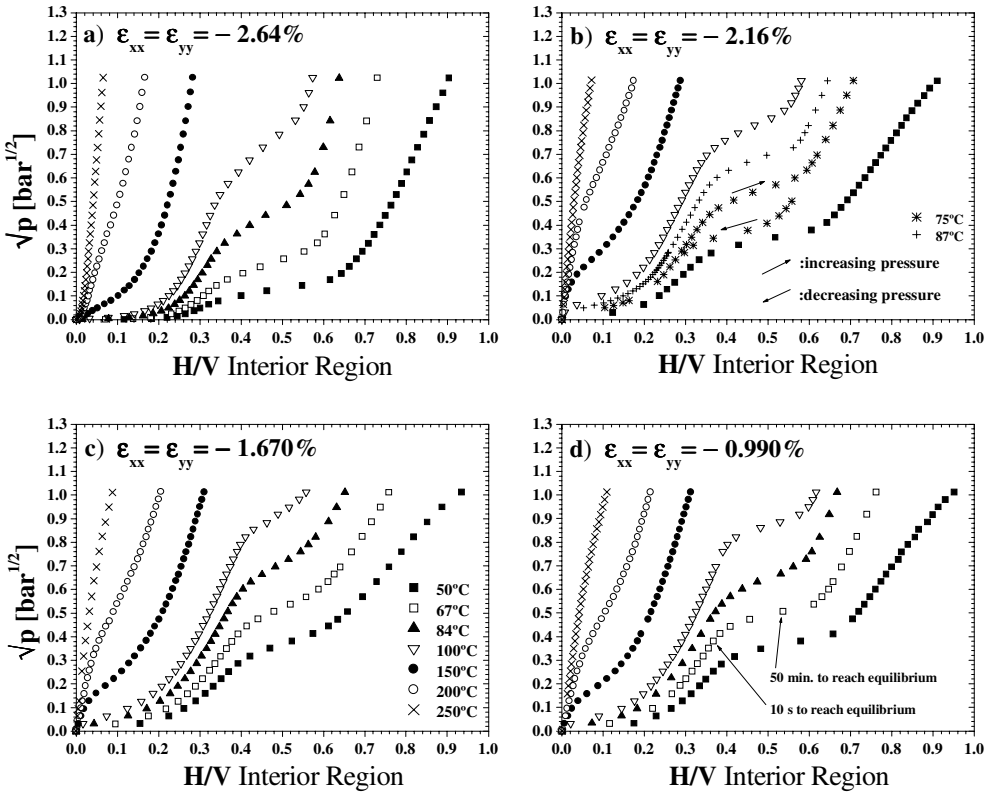

Figure 3. Solubility isotherms for hydrogen in four different Fe/V (001) superlattices. The thickness of the hydrogen-containing vanadium layers is kept constant while the thickness of the hydrogen-free iron layers is varied from 3 to 13 monolayers. This will result in different strain states of the V layers. (a) $\epsilon_{xx} = \epsilon_{yy} = -2.64\%$. (b) $\epsilon_{xx} = \epsilon_{yy} = -2.16\%$. (c) $\epsilon_{xx} = \epsilon_{yy} = -1.67\%$. (d) $\epsilon_{xx} = \epsilon_{yy} = -0.99\%$. The film plane is parallel to the x–y plane.

when the hydrogen is removed from the sample. However, there is a concentration region where the isotherms exhibit hysteresis, as indicated by the arrows in figure 3(b). At low concentrations, there is a clear tendency for increasing solubility with decreasing initial strain (thinner Fe layers). At two different concentrations, the shapes of the isotherms exhibit signs of a phase boundary, the first at the inflection points $c_{c,1} \simeq 0.04$–0.07 and the second at the onset of the plateau region of the isotherms $c_{c,2} \simeq 0.35$. The existence of the first phase boundary was previously observed by Andersson *et al* [8], while the second phase boundary has not been found in earlier studies of H in Fe/V superlattices.

The time to reach equilibrium in the plateau region is typically more than two orders of magnitude larger than at other concentrations (see figure 3(d)), which strongly supports an assignment of ordering. However, no long-range ordering is conceivable due to the absence of a maximum in the measured resistivity. The transition exhibits hysteresis and there is no evidence of any asymptotic trend of the compressibility when the temperature is decreased.

By plotting $\ln\sqrt{p}$ versus $1/T$ at constant c, for the isotherms, $\Delta\bar{H}_{\mathrm{H}}$ and $\Delta\bar{S}_{\mathrm{H}}$ can be obtained by using the van't Hoff relation for solid solutions of H in metals [17]:

$$\ln\sqrt{p} = \frac{\Delta\bar{H}_{\mathrm{H}}}{k_{\mathrm{B}}T} - \frac{\Delta\bar{S}_{\mathrm{H}}}{k_{\mathrm{B}}} \tag{6}$$

where p (atm) is the hydrogen-gas pressure, k_B the Boltzmann constant, $\Delta\bar{H}_H$ the change of enthalpy and $\Delta\bar{S}_H$ the change of entropy. The two latter quantities refer to the differences with respect to the gas phase at 1 atm. The van't Hoff relation is valid in the concentration region of continuous solubility. The upper limit for determination of $\Delta\bar{H}_H$ and $\Delta\bar{S}_H$ is then the phase boundary of the ordered phase: $c_{c,2} = 0.35$. $\Delta\bar{H}_H$ is plotted in figure 4 for the four superlattices in the region $0 < c \leqslant 0.35$ and $\Delta\bar{S}_H$ plotted for one of the superlattices is shown in figure 5(a); the data are also compared to those for H in bulk V. The change of $\Delta\bar{H}_H$ with H concentration is due to an effective H–H interaction. A negative slope corresponds to an attractive interaction and a positive slope to a repulsive interaction. The results for $\Delta\bar{H}_H$ clearly show that the interaction is attractive up to $c \simeq 0.1$ (equal for all strain states), where the attractive interaction is balanced by a repulsive one. In the region $0.1 \leqslant c \leqslant 0.35$ the repulsive interaction dominates; this is in stark contrast with the situation in bulk V and Mo/V superlattices [9], where the interaction is attractive, but in agreement with the results reported by Andersson *et al* [8]. The results for $\Delta\bar{S}_H$ reveal a more ordered H lattice gas in the superlattices than in bulk V, throughout the measured concentration range. The initial loss of entropy from the gas phase up to $c \simeq 0.1$ is significantly larger than in both bulk V and Mo/V superlattices [9, 19]. Similarly to the case for $\Delta\bar{H}_H$, there is a minimum of $\Delta\bar{S}_H$ at $c \simeq 0.1$, and in the region of repulsive interaction: $0.1 \leqslant c \leqslant 0.3$ (see above), $\Delta\bar{S}_H$ increases slightly with concentration.

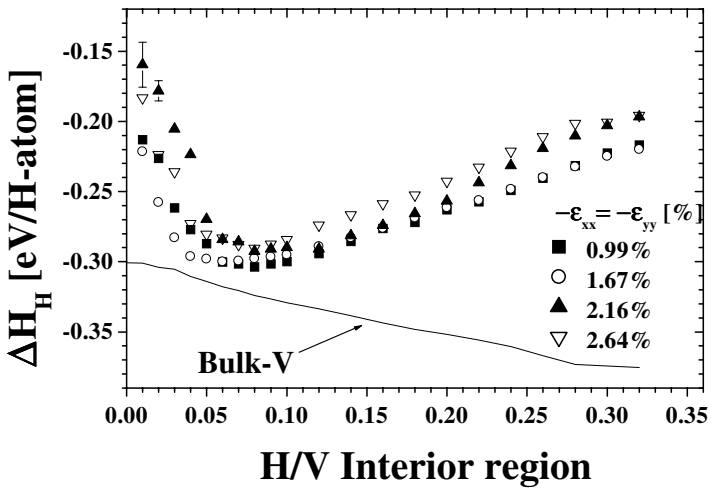

Figure 4. Enthalpy of a solution of hydrogen in Fe/V(001) superlattices. The different plots correspond to different strain states of the hydrogen-containing V lattice.

4. Discussion

Due to the reversibility of the resistance change during hydrogen cycling (loading–unloading), the phase transitions discussed in this article are best represented by coherent transitions. Incoherent lattice-gas → lattice-liquid transitions are associated with creation and motion of dislocations and if a phase transition of this kind had occurred, the resistance change would not have been reversible. At low concentrations (H/V < 0.3), the overall changes in entropy and enthalpy are consistent with the previous investigations of H in Fe/V(001) superlattices [8]. Hence, the details of the uptake with respect to the strain state should be representative for

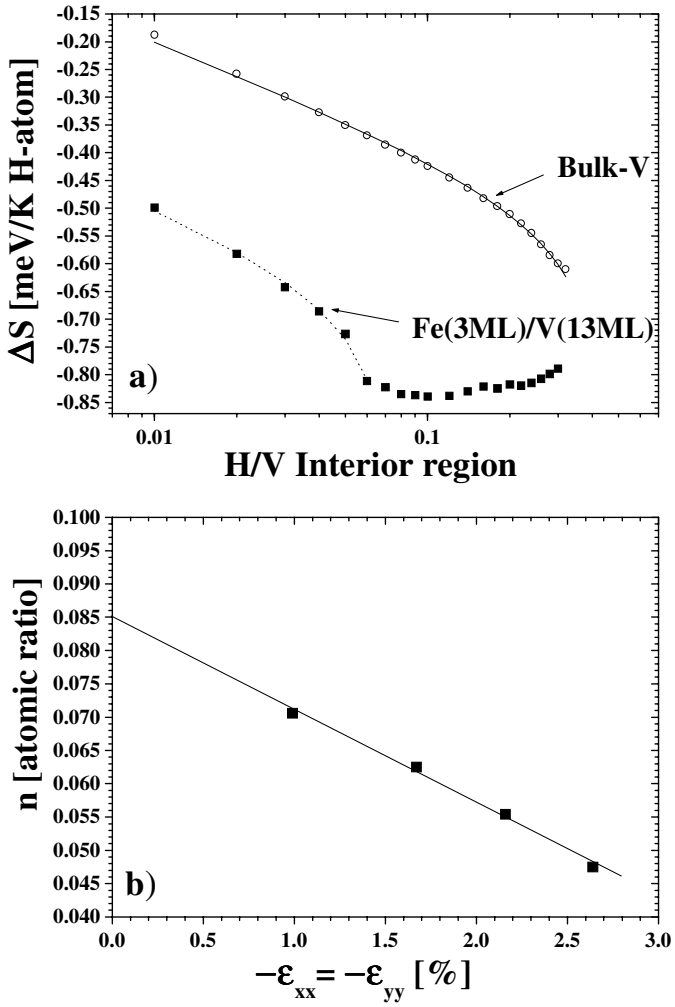

Figure 5. (a) $\Delta\bar{S}_{\mathrm{H}}$ for the solution of hydrogen in an Fe(9 ML)/V(13 ML)(001) superlattice. The entropy changes are fitted with the expression described in the discussion section. (b) The number of sites per V atom available for occupation of H atoms as a function of compressive strain of the host V cell. The range of the repulsive forces scales linearly (solid line) with the strain. Extrapolating to zero strain yields $n = 0.085(1)$, which is five times smaller than in the bulk V–H system.

superlattices of this type. The thermodynamics of H in the clamped hydrogen-dissolving V layers in Fe/V superlattices is expected to be quite different compared to that of a free-standing film or bulk V. Apart from considerable finite-size effects due to the quasi-two-dimensional character of the host lattice, the electronic and elastic boundary conditions as well as the strain state are important for the hydrogen uptake. The electronic boundary conditions are clearly affected by the thickness of the Fe layers and this has consequences for the extent of the hydrogen-depleted regions near the Fe–V interface (see above and reference [11]). Furthermore, the existence of hydrogen-free Fe layers, in combination with a strong adhesion to the substrate, will effectively hinder any H-induced expansion of the V layers in the film plane (x- and y-direction). All expansion due to H occurs in the direction perpendicular to the

film plane (z-direction). This will affect the H–H interaction, which is closely linked to the volume change of a crystal. The 1D expansion will mediate a H–H interaction, which in the extreme case can be purely attractive in the x- and y-directions and purely repulsive in the z-direction (completely polarized elastic dipoles). For more detailed information on this subject, see a recent review article by Zabel and Hjörvarsson [20]. In the following subsections we will discuss the relation between the strain state and the hydrogen absorption, with an emphasis on the phase transitions and the blocking mechanism at low concentrations.

4.1. Low concentration $c < 0.1$

In the limit of an infinitely diluted solution, the phase assignment is of the lattice-gas type with a random distribution of the H atoms over all possible interstitial sites. The initial tetragonal distortion will increase the occupation probability of the O_z sites (the x- and y-directions are parallel to the film plane). The 1D expansion of the film will however completely polarize all H atoms in the z-direction at finite H concentration. The exclusive population of O_z sites is confirmed by x-ray measurements performed by Andersson *et al* [15] and by EXAFS measurements by Burkert *et al* [21].

The apparent strong attractive H–H interaction in the low-concentration range can partly be understood in the terms of gigantic lattice expansion. The absorption potential for H in 3d metals is closely related to the average interstitial electron density (IED). Using the expansion coefficient determined by Andersson *et al* [15], it was possible to estimate the change of volume, and thereby the maximum change in the IED, when the H concentration is increased from 0 to 0.1 (atomic ratio). The resulting volume expansion is 3.5%. The difference in absorption potential can thereby be estimated by using the effective-medium approach of Nörskov [22]. A change in average interstitial electron density (IED) will cause a change in the binding energy of the H atoms corresponding to

$$\delta E = (796\bar{n}_0 + 20.8)\,\delta\bar{n}_0 \tag{7}$$

where δE is the binding energy and $\bar{n}_0$ is the average IED. The average IED of V is well known [23], 0.03 electrons au^{-3}. Ignoring the contribution of H to the IED, the volume change will increase the binding energy by $\simeq$47 meV/H atom. This value should be compared with the change of enthalpy in the present samples, which is at least 90 meV/H atom when the H concentration increases from 0 to 0.1 (atomic ratio). Hence, the change in IED, due to the lattice expansion, cannot alone account for the attractive interaction in the concentration region $0 < c \leqslant 0.1$. Details on the s–d hybridization, as well as the local strain field, are required for quantitative comparison. Furthermore, as the local strain field is apparently important for the interaction energy, changes in the strain state should cause changes in the interaction potential, which will be explored below.

Using the enthalpy data and extrapolating to zero concentration results in $\Delta\bar{H}^0_{\mathrm{H}} = -0.15 \pm 0.02$ eV/H atom for the two samples with the highest initial compressive strain and $\Delta\bar{H}^0_{\mathrm{H}} = -0.20 \pm 0.02$ eV/H atom for the two least strained samples. This is qualitatively in line with the expected tendency, as increased compressive strain increases the electron density, which results in less-energetic absorption. However, as stated above, the energy of the local strain field is unknown, which prohibits quantitative comparison.

By treating the absorbed H atoms as a lattice gas, it is possible to extract the compressibility from the isotherms. The inverse of the compressibility, κ^{-1}, is proportional to $c^2T\,\partial(\ln p)/\partial c$ [24]. Figure 6 reproduces the temperature dependence of κ^{-1} at $c_{\mathrm{c},1}$, which clearly reveals a Curie–Weiss behaviour. The corresponding critical temperature was found by extrapolating linear fits of the data down to $\kappa^{-1} = 0$. The critical temperature was found to be 43($\pm$2) °C;

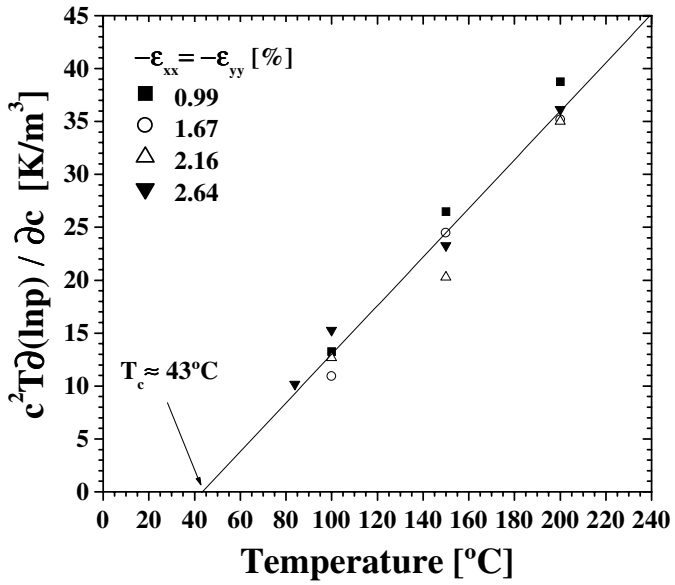

Figure 6. The divergence of the compressibility of the hydrogen lattice gas at the critical concentration $c_{c,1} = 0.03$–0.07 (atomic ratio) for different initial strain states of the hydrogen-containing V layer in Fe/V(001) superlattices. The behaviour is clearly of the Curie–Weiss type and independent of the strain state.

no significant influence of different strain states was noticed. The concentration at the first inflection point, $c_{c,1}$, is temperature dependent, varying from $c \simeq 0.04$ at 100 °C to $c \simeq 0.07$ at 200 °C, at variance with the results reported by Andersson *et al* [8]. Hence, the interaction is clearly manifested in a phase boundary, which shows similar asymptotic behaviour to H in Nb at the $\alpha \rightarrow \alpha'$ phase boundary; no corresponding continuous transition has been observed in the bulk V–H system; see reference [26] and references therein.

To investigate the uniqueness of the quasi-two-dimensional host, we now explore the influence of the finite size and the strain state on the phase boundaries. The strain state was previously found to strongly alter the site occupancy of H—see [10] and references therein—as for example is seen in comparing Mo/V(001) and Fe/V(001) superlattices. The change of site does completely change the symmetry of the local strain field; hence the interaction potential should be strongly altered. One manifestation of the interaction is an onset of blocking in the hydrogen-absorbing host. To study this possibility further, we regard the changes of the entropy in the dilute limit and discuss the blocking which enters the expression for describing the configuration entropy of the lattice gas. The partial molar entropy of H in a metal lattice can be divided into two terms:

$$\bar{S}_{\mathrm{H}} = \bar{S}^{\mathrm{c}} + \bar{S}^{\mathrm{nc}} \tag{8}$$

where $\bar{S}_{\mathrm{c}}$ is the configurational term and $\bar{S}_{\mathrm{nc}}$ is the non-configurational term. In the ideal case (i.e. H atoms randomly distributed over all possible sites), the configurational term is equal to

$$\bar{S}^{\mathrm{c,ideal}} = k_{\mathrm{B}} \ln \left[\frac{n-c}{c} \right] \tag{9}$$

where n is the number of sites per V atom available for H atoms. In group-Vb metals, H atoms normally populate tetrahedral sites, which implies $n = 6$. The experimentally determined entropy of H in bulk V exhibits a big deviation from the ideal case, which has been treated by

different blocking models; i.e. the presence of a H atom blocks the neighbouring interstitial sites for occupation by another H atom [25]. Focusing on the concentration region below $c_{c,1}$, this approach can be utilized in the present discussion. It is reasonable to ignore the concentration dependence of $\bar{S}^{nc}$ in the low-concentration range, as all of the samples under study are expected to contribute equally. The following expression can thus serve as a model for the entropy change:

$$\Delta\bar{S}_H = k_B \ln\left[\frac{n-c}{c}\right] + \Delta\bar{S}^{nc} \tag{10}$$

where n and $\Delta\bar{S}^{nc}$ can be regarded as fitting parameters. The best fit to the entropy data in the concentration region below $c_{c,1}$ is presented in table 2 and is also shown, for one of the superlattices, in figure 5(a). As a comparison, the best fit of equation (10) to the entropy data for bulk V of Waleckis and Edwards [19] is also included. Note that the blocking concentrations represent two different phases, $\alpha \rightarrow \beta$ in the bulk and $\alpha \rightarrow \alpha'$ in the extremely thin V layers. As seen in figure 5(b), the blocking concentration is found to scale linearly with the strain field. Extrapolating to zero strain yields $n = 0.085(1)$ (atomic ratio), which is a factor of 5 smaller than the blocking seen in bulk V. The dependence of the blocking range on the strain field is also observed in the solubility isotherms. Hence, the thermodynamics of the absorbing layers are strongly affected by both their finite extent and their initial strain state.

Table 2. The best fit to the expression $\Delta\bar{S}_H = k_B \ln[(n-c)/c] + \Delta\bar{S}^{nc}$, where $\Delta\bar{S}^{nc}$ and n are the fitting parameters and c is the atomic ratio, of the entropy data for the superlattices at low concentrations. The best fit to the bulk V entropy data of Waleckis and Edwards [19] is also included for comparison. The blocking concentration scales linearly with the strain (see figure 5(b)).

$-\epsilon_{xx} = -\epsilon_{yy}$ (%)	$\Delta\bar{S}^{nc}$ (meV K^{-1}/H atom)	n (atomic ratio)
2.64	−0.59(3)	0.047(5)
2.16	−0.57(7)	0.055(4)
1.67	−0.69(4)	0.062(5)
0.99	−0.66(0)	0.070(6)
Bulk V, reference [19]	−0.52(0)	0.415(9)

4.2. Intermediate and high concentrations $c \geqslant 0.1$

In the concentration range $0.1 \leqslant c \leqslant 0.35$, the repulsive interaction between the H atoms dominates over the attractive one. The phase assigned for the H atoms in this region can best be described as an anisotropic liquid, where the interaction is attractive in the film plane and repulsive out of the plane; see Andersson *et al* [18]. No blocking is evident in the entropy data in this concentration range.

The plateau region of the isotherms starts at $c_{c,2} \simeq 0.35$ and is independent of both the initial strain field and temperature. The change of time constant of the kinetics and the hysteresis, which is associated with the plateau region, strongly indicates that ordering of the H atoms is taking place. The asymptotic behaviour of the isotherms after the transition suggests formation of a hydride with the composition VH. There is no information available regarding the structure of hydrides in Fe/V superlattices; only local order has been determined. However, assuming exclusive octahedral occupancy, a hard-core blocking must exist when $c > 1$. A comparison with the phase diagram of H in bulk V is therefore possible [26]. The onset of the two-phase region (α- and β-phases) in the bulk VH_c system is already occurring at $c = 0.1$ at 100 °C. This implies the corresponding phase boundary being suppressed up to $c \simeq 0.35$

in the Fe/VH_c system. By plotting ln p versus $1/T$ for the isotherms in the plateau region, it is possible to determine the phase formation energy for the $\alpha' \rightarrow \beta$ transition. The values obtained, around -0.18 eV/H atom, are approximately the same for all samples; the value for bulk V is -0.16 eV/H atom [26].

5. Summary and conclusions

The thermodynamics for H atoms absorbed in Fe/V superlattices with different initial strain states of the H-dissolving V layers are presented. The change of $\Delta\bar{H}_{\mathrm{H}}$ with H concentration indicates an attractive H–H interaction up to $c \simeq 0.1$, and a repulsive interaction at higher concentrations. Varying the biaxial initial compressive strain from $\epsilon_{xx} = \epsilon_{yy} = -0.99$ to -2.64% (the x- and y-direction are parallel to the film plane) proves to have a small impact on the long-ranged attractive interaction between the H atoms. However, the range of the repulsive interaction was found to scale linearly with the initial strain. From the solution isotherms it is clear that the Fe/VH_c system undergoes two phase transitions in the region $50 \leqslant T \leqslant 300\ ^{\circ}\mathrm{C}$ and $0 < c \leqslant 1$. The first transition shows a Curie–Weiss-like behaviour and can at this point be described as a lattice-gas $\rightarrow$ anisotropic liquid transition with the attractive interaction direction parallel to the film plane and repulsive interaction in the direction perpendicular to the film plane. The second transition resembles a disorder $\rightarrow$ (local) order transition and is accompanied by hysteresis. The phase boundary at $c \simeq 0.35$ was found to be unaffected when the compressive strain varied from $\epsilon_{xx} = \epsilon_{yy} = -0.99$ to -2.64%.

Acknowledgments

This work was financially supported by the Swedish Natural Science Research Council (NFR). The authors would like to thank H Zabel at Ruhr-Universität Bochum for valuable discussions.

References

[1] Huiberts J, Griessen R, Rector J, Dekker J, de Groot D and Koeman N 1996 *Nature* **380** 281
[2] Hjörvarsson B, Dura J, Isberg P, Watanabe T, Udovic T, Andersson G and Majkrzak C 1997 *Phys. Rev. Lett.* **79** 901
[3] Wagner H and Horner H 1974 *Adv. Phys.* **23** 587
[4] Alefeld G 1972 *Ber. Bunsenges. Phys. Chem.* **76** 746
[5] Alefeld G 1971 *Critical Phenomena in Alloys, Magnets and Superconductors* ed R E Mills (New York: McGraw-Hill)
[6] Zabel H and Peisl H 1980 *Acta Metall.* **28** 589
[7] Steyrer G and Peisl H 1986 *Europhys. Lett.* **2** 835
[8] Andersson G, Hjörvarsson B and Isberg P 1996 *Phys. Rev.* B **55** 1774
[9] Stillesjö F, Ólafsson S, Isberg P and Hjörvarsson B 1995 *J. Phys.: Condens. Matter* **7** 8139
[10] Hjörvarsson B, Andersson G and Karlsson E 1997 *J. Alloys Compounds* **253** 51
[11] Hjörvarsson B, Ryden J, Karlsson E, Birch J and Sundgren J-E 1990 *Phys. Rev.* B **43** 6440
[12] Birch J, Sundgren J E and Fewster P 1995 *J. Appl. Phys.* **78** 6562
[13] Isberg P, Hjörvarsson B, Wäppling R, Svedberg E and Hultman L 1997 *Vacuum* **48** 483
[14] Ostanin S, Uzdin V, Demangeat C, Wills J, Alouani M and Dreysse H 2000 *Phys. Rev.* B **61** 4870
[15] Andersson G, Hjörvarsson B and Zabel H 1997 *Phys. Rev.* B **55** 15 095
[16] Hjörvarsson B, Birch J, Stillesjö F, Ólafsson S, Sundgren J E and Karlsson E 1997 *J. Phys.: Condens. Matter* **9** 73
[17] Flanagan T and Oates W 1972 *Ber. Bunsenges. Phys. Chem.* **76** 706
[18] Andersson G, Andersson P H and Hjörvarsson B 1999 *J. Phys.: Condens. Matter* **11** 6669
[19] Waleckis E and Edwards R K 1996 *J. Phys. Chem.* **9** 73
[20] Zabel H and Hjörvarsson B 2001 Progress in hydrogen treatment of materials, at press

[21] Burkert T, Miniotas A and Hjörvarsson B 2001 *Phys. Rev.* B at press
[22] Nörskov J 1982 *Phys. Rev.* B **26** 2875
[23] Papadia S, Karlsson K, Nilsson P and Jarlborg T 1992 *Phys. Rev.* B **45** 1857
[24] Griessen R 1999 *The Physics of Hydrogen in Metals* (Amsterdam: Vrije Universiteit)
[25] Oates W, Lambert J and Gallagher P 1969 *Trans. Metall. Soc. AIME* **245** 47
[26] Shoeber T 1996 *Hydrogen Metal Systems I* ed F Lewis and A Aladjem (Zurich: Scitec)